



저작자표시-비영리-변경금지 2.0 대한민국

이용자는 아래의 조건을 따르는 경우에 한하여 자유롭게

- 이 저작물을 복제, 배포, 전송, 전시, 공연 및 방송할 수 있습니다.

다음과 같은 조건을 따라야 합니다:



저작자표시. 귀하는 원저작자를 표시하여야 합니다.



비영리. 귀하는 이 저작물을 영리 목적으로 이용할 수 없습니다.



변경금지. 귀하는 이 저작물을 개작, 변형 또는 가공할 수 없습니다.

- 귀하는, 이 저작물의 재이용이나 배포의 경우, 이 저작물에 적용된 이용허락조건을 명확하게 나타내어야 합니다.
- 저작권자로부터 별도의 허가를 받으면 이러한 조건들은 적용되지 않습니다.

저작권법에 따른 이용자의 권리는 위의 내용에 의하여 영향을 받지 않습니다.

이것은 [이용허락규약\(Legal Code\)](#)을 이해하기 쉽게 요약한 것입니다.

[Disclaimer](#)

공학석사 학위논문

**Searching for a new organic-based electrolyte
with highly stable and efficient Li/O₂ battery**

고효율 리튬/공기 전지를 위한 새로운
유계 전해질 탐구에 관한 연구

2019년 2월

서울대학교 대학원

재료공학부

박 승 관

Abstract

Searching for a new organic-based electrolyte with highly stable and efficient Li/O₂ battery

PARK, Sung Kwan

Department of Material Science and Engineering

College of Engineering

The Graduate School

Seoul National University

Lithium oxygen battery holds the greatest promise for the future energy applications due to its high theoretical capacity¹. However, several critical challenges remain due to the instability of reduced oxygen species (O₂⁻) which causes detrimental side-reaction with the organic electrolyte²⁻⁶. Moreover, the stability of Li metal with the currently used organic solvents in Li-O₂ causes dendritic growth upon cycling due to the formation of inhomogeneous solid electrolyte interphase⁵. In this thesis, we proposed a list of new solvents for the candidates towards highly stable electrolytes in Li-O₂ batteries. The stability of various solvents towards O₂⁻ and Li metal were verified using chemical and electrochemical investigations and their

feasibility for Li-O₂ cells has been demonstrated. Through comparative study, proposed electrolyte has been found to have comparable stability towards O₂⁻ and unexpectedly profound stability towards Li metal. Nevertheless, the cycle performance demonstrates that the severe accumulation of side-products accumulated upon cycling which led to cell death. Hence, the importance of stabilizing O₂⁻ for highly efficient Li-O₂ battery has been emphasized through this work.

Keywords: Li-O₂ battery; Organic electrolyte; Aprotic Li-O₂; O₂⁻ stability; Li metal stability

Student Number: 2016-28630

Contents

Abstract	i
List of Figures	v
Chapter 1. Introduction	1
1.1 Motivation	1
Chapter 2. Research backgrounds	4
2.1 Lithium Rechargeable battery	4
2.2 Lithium-Oxygen battery	6
Chapter 3. Experimental section	10
3.1 Electrochemical analysis	10
3.2 Ex-situ structural analysis.....	11
3.2.1 X-ray diffraction.....	11
3.2.2 Field emission scanning electron microscope.....	11
3.2.3 Fourier transform infrared spectrometry	12
3.3 Differential Electrochemical Mass Spectroscopy.....	12
3.4 Quantitative analysis of discharge product.....	12
3.4.1 UV-vis spectroscopy	12
3.4.2 Iodometric titration technique	13

Chapter 4. Results and Discussions	14
4.1 Physical and Electrochemical properties of solvent candidates	14
4.2 Chemical and Electrochemical stability of Dioxane with Li metal....	18
4.3 Electrochemical profile and discharge product analysis of Dioxane .	24
4.4 Qualitative and Quantitative study of the discharged products	29
4.5 Cycle performance of Dioxane electrolyte in Li-O ₂ cell.....	37
Chapter 5. Conclusion	41
Reference	42

List of Figures

Figure 1.1 Strategy for designing new electrolyte for Li-O₂ system.

Figure 2.1 Schematic figure for the fundamental of lithium-based rechargeable battery.

Figure 2.2 Schematic figure for the fundamental of Li-O₂ rechargeable battery.

Figure 4.1 B.P and M.P of solvent candidates. Solubility check with 0.1M LiTFSI in solvents at 60°C (right). Up to 0.5 M LiTFSI in Dioxane solution could be prepared in 40°C.

Figure 4.2 Physical property comparison of Dioxane with the most commonly used electrolytes in Li-O₂ system.

Figure 4.3 Linear sweep voltammetry (LSV) performed using the Three-electrode cell within the 0–5.0 V vs. Li/Li⁺ range at 1.0 mV s⁻¹ at 40°C.

Figure 4.4 Photographs of Li metal immersed in 0.5 M LiTFSI Dioxane, DME, TEGDME at 40°C over storage time.

Figure 4.5 Comparison of the voltage profiles of the Li/Li symmetric cell with 0.5 M LiTFSI TEGDME, DME and Dioxane.

Figure 4.6 Comparison of the voltage profiles of the Li/Li symmetric cell with 0.5 M LiTFSI Dioxane in Ar and O₂ atmosphere.

Figure 4.7 SEM images of the surface morphologies of lithium metals (a,b) in 0.5 M LiTFSI TEGDME after 60 cycles, (c,d) in 0.5 M LiTFSI DME after 130 cycles at a current density of 0.5 mA cm^{-2} .

Figure 4.8 Electrochemical profile of Li-O₂ cell using 0.5 M LiTFSI in Dioxane at 0.1 mA cm^{-2} at 40°C . The dotted line indicate the theoretical formation voltage of Li₂O₂. Purple and Pink circles indicate the full discharge and full charged state of the cell, respectively.

Figure 4.9 Ex situ XRD patterns of Li-O₂ cells using 0.5 M LiTFSI Dioxane: after discharge, and charge.

Figure 4.10 FTIR spectra of Ketjen Black cathode in 0.5 M LiTFSI in Dioxane after discharge and charge under O₂ between 2 and 4.5 V vs. (Li/Li⁺).

Figure 4.11 FE-SEM images of the air electrode: pristine (a),and after discharge (b) and re-charge (c) at the same magnification.

Figure 4.12 UV-vis spectra for qualitative analysis of the Li₂O₂ yield in DME, Dioxane, TEGDME. Yellow dotted line indicates the $[\text{Ti}(\text{O}_2^{2-})]^{2+}$ complex due to the presence of H₂O₂ ($\sim 407\text{nm}$).

Figure 4.13 The yield of Li₂O₂ as measured by iodometric titration in different electrolytes. The yield is presented as the percentage of the expected theoretical amount on the basis of the e⁻ passed. Data are represented as mean \pm standard

deviation.

Figure 4.14 Direct comparison of the CO₂ evolution from decomposition of Li₂CO₃ (formed from decomposition of the electrolyte). H⁺ indicates the time H₃PO₄ added and the evolve gas is CO₂ from Li₂CO₃.

Figure 4.15 In situ DEMS analyses using Dioxane, DME and TEGDME.

Figure 4.15 Cycling curves and capacity retention of DME, Dioxane and TEGDME Li-O₂ cell. a,b,c Galvanostatic discharge/charge cycles recorded in 0.5M LiTFSI in DME, Dioxane and TEGDME at 0.1 mA cm⁻². d,e,f Capacity retention for the same cell as in a,b,c.

Figure 4.17 Cycling curves of DME, Dioxane and TEGDME Li-O₂ cell. Rebuilt with a fresh Li metal.

Figure 4.18 FE-SEM images of the air electrode: pristine (a), and after discharge (b) and after 15 cycles (c) at the same magnification.

Chapter 1. Introduction

1.1 Motivation

Metal-air batteries, due to their high theoretical energy density (~2-10 folds higher than those of lithium-ion batteries), received tremendous attention and dedication to improve its performance for future energy applications⁷. Among the various types of metal-air batteries, Li-air batteries have received revived interest due to their high theoretical energy densities (~3500 W h kg⁻¹), which are among the highest for known battery chemistries². However, several critical challenges such as cathode pore clogging, electrolyte instability, degradation of the air cathode hinder the development of such a technology^{2, 8, 9}. To resolve these challenges, many researches have been focused on to elucidate the origin of these issues by investigating the reaction mechanism of oxygen reduction and oxygen evolution reaction of the system^{2, 4, 6, 10, 11}.

The ideal reaction of Li-O₂ batteries is based upon the electrochemical formation (discharge) and decomposition (charge) of lithium peroxide (Li₂O₂). The discharge reaction undergoes the formation of strong nucleophile oxygen radical (O₂⁻) which readily form intermediate species LiO₂ with Li⁺ follow by reaction to form Li₂O₂, or attack carbon atom of the solvent molecules through nucleophilic attack or H-abstraction (side reaction)^{1, 8}. In contrast, the charge reaction undergoes direct decomposition of Li₂O₂ without generating O₂^{-1, 8}.

Studies has proved that O_2^- the strong nucleophile are energetically favorable to attack the electron-deficient part of the solvent forming a $[\text{solvent-O}_2]^-$ complex and hence consumes the electrolyte during cell operation^{10, 12, 13}. Previous reports, both theoretical and experimental observation has suggested that the solvents acidity, solvating ability and the formation energy for $[\text{solvent-O}_2]^-$ complex can be indicators to find a stable electrolyte towards the reactive oxygen species¹⁰. Nevertheless, the organic electrolytes reported in Li-O₂ exhibit poor cycle performance and far from realization of long-life Li-O₂ batteries^{3, 14}. Hence, the identification of a new electrolyte that exhibits high stability against the nucleophilic attack of oxygen radicals are indispensable for long-life Li-O₂ batteries.

Here, we propose a list of new solvents for the candidates towards highly stable electrolytes in Li-O₂ batteries. With the aid of theoretical calculation, three electrolytes that have not been reported could be found. The stability of various solvents towards ROS and Li metal has been verified using chemical and electrochemical approach and their feasibility in Li-O₂ cells has been demonstrated.

Reported solvents for Li-O₂ batteries

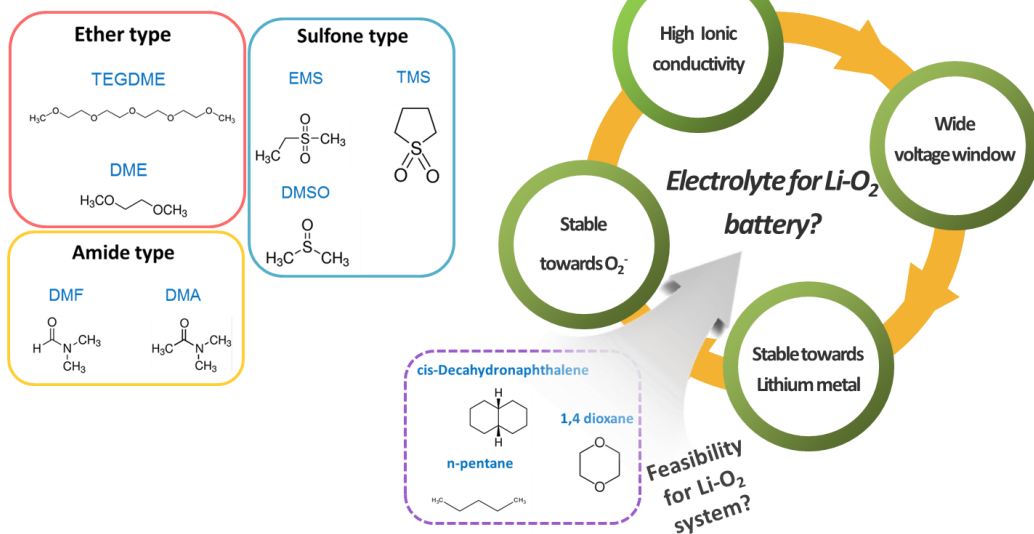


Figure 1 Strategy for designing new electrolyte for Li-O₂ system

Chapter 2. Research backgrounds

2.1 Lithium Rechargeable Batteries

Recently, due to the exhaustion of renewable energies and the increasing demand of portable device and energy storage system (ESS), designing of high energy density system with good sustainability is required^{1, 8, 9}. To use high technology portable devices, rechargeable batteries has been widely known as having high energy density and power capability^{1, 8, 9}. Among various rechargeable batteries, lithium-based rechargeable batteries have shown remarkable performance⁷. Discharge voltage and energy density of lithium rechargeable batteries are approximately 3.7 V and 150 Wh kg⁻¹, respectively, which are much higher than those of other rechargeable battery system⁷.

Basic principle of lithium rechargeable batteries is shown in Figure 2.1. Lithium rechargeable batteries are composed of anode, electrolyte, cathode, and separator. During the discharge reaction, lithium ions diffuse out from the anode (typically graphite) to cathode (typically LiCoO₂) through the liquid electrolyte and electrons from the anode (oxidized) move to cathode through an external circuit spontaneously. In contrast, lithium ions and electrons move back to anode during the charge reaction and since this process is not a spontaneous reaction, electrical energy is required for the reverse reaction to occur. Since the overall discharge and charge undergoes the conversion of chemical energy to electrical energy, the entire reaction

of battery system is widely known as electrochemical reaction.

The electrochemical reaction of conventional Li-ion rechargeable battery with graphite (anode) and LiCoO_2 (cathode) during discharge/charge are expressed as follow:



The energy that can be stored in a battery can be determined by the specific capacity and the voltage. The specific capacity indicates the amount of electrons that can be stored in anode/cathode per unit weight, and the voltage is determined by the difference in Li chemical potential between the cathode and anode.

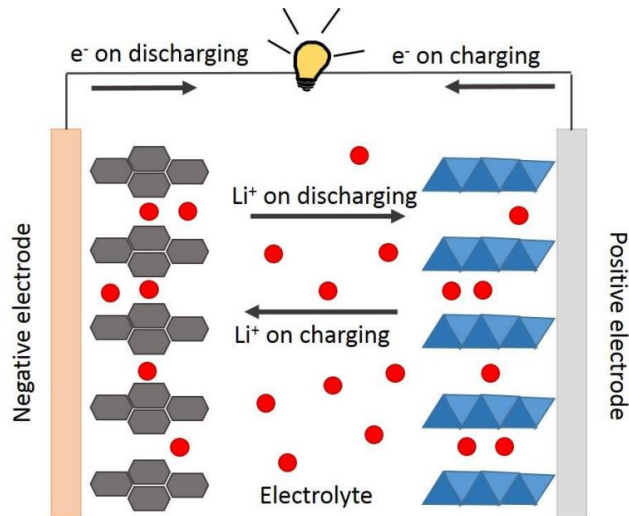
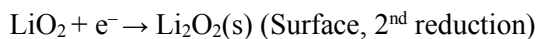
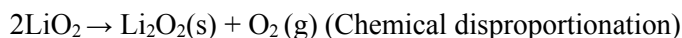
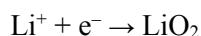
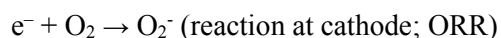
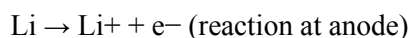


Figure 2.1 Schematic figure for the fundamental of Li-ion rechargeable battery with graphite as anode (Negative electrode) and LiCoO₂ as cathode (Positive electrode)¹⁵.

2.2.2 Lithium-oxygen batteries

Since the first report of polymer-electrolyte based Li-O₂ battery by Abraham *et. al* (1996), Li-O₂ battery has been studied intensely¹⁶. The reactants of Li-O₂ system is O₂ derived from air, which is an abundant resource and freely available outside which makes the battery with one of the highest theoretical energy. Li-O₂ cells typically consist of metallic Li as the negative electrode, a porous air electrode on the positive side and a Li⁺ conducting electrolyte which can be aqueous, aprotic, a mixture of aqueous and aprotic, or solid-state. A simple schematic of Li-

O₂ cell is shown in Figure 2.2. The working principle of Li-O₂ battery simply undergoes the diffusion of O₂ from outside towards porous electrode and dissolves into the electrolyte where it is reduced during the discharge reaction. In aprotic electrolytes, the two possible reductions may proceed through the mechanisms listed below^{1, 13}.



During the charge reaction, the reverse reaction occurs where O₂ is released from the positive electrode and the Li⁺ is plated back onto the metallic Li. Although Li-air batteries have the energy storage advantages over many other rechargeable system including other post-LiB, many challenges still remain. Li-O₂ combines two challenging electrodes, Li metal and O₂. Li-metal electrodes have been investigated for many years and still do not delivery the necessary cycle life due to inhomogeneity of Li deposition/plating. Moreover, the electrochemical reaction of Li-O₂ is often

problematic since the first reduced species during the discharge is O_2^- , a well-known nucleophile readily reacts with all of the battery components in Li-O₂. Hence, following issues must be considered in order to realize highly efficient Li-O₂ battery:

1. Finding an aprotic electrolyte with good stability towards O_2^- ;
2. Finding ways to minimize dendrite formation of Li metal;
3. Minimizing the carbon degradation which occurs during the charge (above 3.5 V vs. Li/Li⁺)

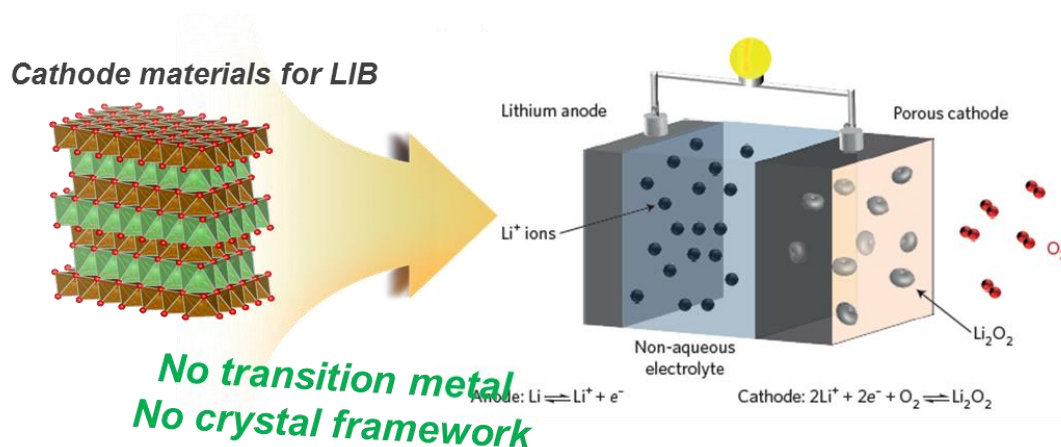


Figure 2.2 Schematic figure for the fundamental of Li-O₂ rechargeable battery⁸.

The former two is of central interest to this thesis. The severe side reaction between battery components and the O_2^- produces electrically insulating products (Li_2CO_3 , etc) which ultimately affects the overpotential and cycle life over repeated

cycles¹. Since the dissolved O₂ in the electrolyte is reduced first during the discharge, the energetics between solvent molecules and O₂⁻ is critical. In order to proceed a comparative study for electrolytes with a good O₂⁻ stability, well simplified experimental model system is essential. In this thesis, a comparative study of various electrolytes has been conducted through qualitative and quantitative measurements of Li₂O₂ in discharged cathode. The Li₂O₂ yield in the discharged cathodes dictates the amount of reduced oxygen species (O₂⁻) transformed to Li₂O₂ with respect to the charge transferred during the discharge. Therefore, by quantifying the amount of Li₂O₂, the stability of O₂⁻ towards the cell component can be investigated¹¹. In general, the majority portion of instability of O₂⁻ comes from the side reaction between O₂⁻ and the surrounding solvent, numerous researches have been focused on finding a new type of electrolyte, additives, etc^{1, 2, 8}.

Chapter 3. Experimental section

3.1 Electrochemical analysis

The carbon air cathodes were prepared by the following sequence. A slurry of Ketjen Black carbon paste and polytetrafluoroethylene (60 wt% emersion in water, Sigma-Aldrich) with a mass ratio of 9:1 in a solution of isopropanol (>99.7%, Sigma-Aldrich) and N-methyl-2-pyrrolidone (99.5%, anhydrous, Sigma-Aldrich) with a volume ratio of 1:1 was casted on Ni mesh current collectors. The carbon-coated Ni mesh was dried at 70 °C for overnight in vacuum to completely remove any residual H₂O impurities and the solvent.

The Li–O₂ cells were assembled using a Swagelok-type cell with Li metal anode (300 μm and 20 μm thick), electrolyte soaked separators and carbon cathode (1/2 diameter). The solvent used in this study was 1,4 dioxane (anyhydrous, 99%, Sigma-Aldrich), n-pentane (anhydrous, 99%, Sigma-Aldrich), 1,2-Dimethoxyethane (anhydrous, 99.5%, Sigma-Aldrich), cis-decahydronaphthalene (99%, Sigma-Aldrich), Tetraethylene glycol dimethyl ether (99%, Sigma-Aldrich) and N,N-Dimethylacetamide (99%, Sigma-Aldrich). The solvent without anhydrous label was dried using 3-Å molecular sieves for over 1 week, and the salt (0.5 M LiTFSI) was also kept in a vacuum chamber for the same time before use. The final water content in the electrolyte was < 40 p.p.m. according to a Karl–Fisher titration measurement. The amount of electrolyte used for the cell was 400 μl. Whatman Glass microfiber

filter (GF/F) was used as separator. Electrochemical battery tests of the Li–O₂ cells were conducted using a potentiogalvanostat (WonA Tech, WBCS 3000, Korea). All the cells were relaxed under 770 torr of O₂ pressure at 40 degree Celsius for 1 h before the tests. After being saturated with O₂ gas, the cells were tested for its full discharge and capacity cut cycle life tests.

3.2 Ex-situ structural analysis

3.2.1 X-ray diffraction

After galvanostatic measurements, the cathodes of 0.5 M LiTFSI in 1,4 dioxane were collected from disassembled Li–O₂ cells and washed with 1,2-Dimethoxyethane (>40 p.p.m., 99.8%, Sigma-Aldrich) in a glove box to remove any residual electrolyte. X-ray diffraction spectra of the cathodes were obtained using a Bruker D2-Phaser (Cu K α λ = 1.5406 Å) with the aid of a specially designed airtight holder to prevent outer atmospheric contamination.

3.2.2 Field emission scanning electron microscope

The electrodes were disassembled from the Li-O₂ cell and rinsed with DME solvent in a glove box several times to remove any residual electrolyte. The morphology of the discharged/charged cathodes and Lithium metal anode were observed by Field-emission scanning electron microscopy (FE-SEM; SUPRA 55VP,

Carl Zeiss, Germany). The air cathodes were coated with Pt in prior to the characterization. The sample exposure to the air was minimized to prevent any unwanted decomposition of the sample.

3.2.3 Fourier transform infrared spectrometry

Fourier transform infrared (FTIR; FTIR-4200, JASCO, Japan) spectroscopy analysis was conducted through collecting carbon particles from the carbon cathode and pelletizing the samples with KBr powder.

3.3 Differential Electrochemical Mass Spectroscopy

For the determination of gas evolution during charge, DEMS equipment (HPR-20, Hiden Analytical) connected with a potentiogalvanostat was used. A detailed description of DEMS setup and procedures are provided elsewhere¹⁷.

3.4 Quantitative analysis of discharge product

3.4.1 UV-vis spectroscopy

To qualitatively analyze the amount of Li_2O_2 in the discharge cathode, UV-vis titration using UV-vis spectroscopy (Cary 5000, Agilent, United States) was conducted. The experimental procedure was conducted as previously reported¹⁸.

3.4.2 Iodometric titration technique

To quantitatively analyze the yield of Li_2O_2 , 2 mL of D.I water was injected into the sealed vial using a disposable syringe. The vial contents were then vigorously stirred for ~30 secs, after which the vial was opened and the formed base (due to LiOH) was titrated with a standardized 0.005 M HCl solution (a drop of phenolphthalein in isopropanol is used as the end-point indicator). After the base was titrated, three reagents were added to the existing solution: 1 mL of 2 wt% KI in H_2O , 1 mL of 3.5M H_2SO_4 , and 50 μL of a molybdate-based catalyst solution. The peroxide solution turns yellow upon reagent addition due to I_2 formation, and the I_2 is immediately titrated to a faint straw color using 0.01M NaS_2O_3 . At this point, ~0.5 mL of a 1% starch indicator is added to the solution, which turns dark blue, and the titration is continued until the solution turns clear.

Chapter 4. Results and Discussions

4.1 Physical and Electrochemical properties of solvent candidates

In order to be used as typical Li electrolytes, the solvent candidates must meet the following two major requirements: 1) a solvent must be at its liquid phase within the operation temperature, 2) a solvent must be capable of dissolving Li-containing salt⁷. Figure 4.1 shows the B.P and M.P of the solvent candidates and it is clear that for n-pentane, very low B.P makes it impractical for Li electrolytes. To identify whether the solvent candidates could be the 2nd requirement, a simple experiment has been conducted. One of the most commonly used Li salt, LiTFSI, was chosen to see if the salt is soluble when mixed with the solvents.

Unfortunately, 0.1M LiTFSI in both n-pentane and cis-Decahydronaphthalene were insoluble at room temperature. Similarly, 0.1M LiTFSI in 1,4 dioxane was insoluble at room temperature, but with a slight increase in temperature up to 40°C, clear solution up to 0.5 M LiTFSI in 1,4 dioxane could be achieved. However, both n-pentane and cis-Decahydronaphthalene even at the temperature as high as 60°C could not fully dissolve the salt as shown in Figure 4.1. Hence, it was concluded that both n-pentane and cis-Decahydronaphthalene were inadequate to be used as Li electrolyte and further investigations has only been focused on 1,4 dioxane.

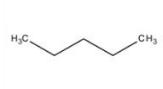
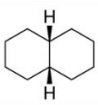
Candidates	B.P. (°C)	M.P. (°C)		
 n-pentane	36.1	-43.1	 0.1M LiTFSI	Salt Insoluble
 cis-Decahydronaphthalene	195.8	-129.8	 0.1M LiTFSI in Deca	Salt Insoluble
 1,4 dioxane	101.3	11.8	 0.1M LiTFSI in dioxane	Soluble at 40°C

Figure 4.1 B.P and M.P of solvent candidates. Solubility check with 0.1M LiTFSI in solvents at 60°C (right). Up to 0.5 M LiTFSI in Dioxane solution could be prepared in 40°C.

Further investigations on physical properties of 1,4 dioxane were conducted and its comparison with the most commonly used solvent, TEGDME and DME is shown in Figure 4.2. The advantage of 1,4 dioxane towards DME solvent is its higher B.P. Therefore, a slightly higher thermal stability of 1,4 dioxane than that of DME is expected. The major disadvantage of 1,4 dioxane could be its low ionic conductivity of 0.51 mS cm^{-1} . The characteristic of having low ionic conductivity may be due to its low dielectric constant, which the low polarity of solvent molecules make it difficult to dissociate the salt cations and anions⁷. However, the low ionic conductivity value within the range of Ionic liquids, its feasibility towards Li-O₂ system has been further investigated^{19,20}.

Figure 4.3 shows the electrochemical stability window of the electrolytes. The shaded region indicates the operational voltage range of Li-O₂ system and clearly, no electrochemical reaction occurs within this range for all the three electrolytes. Moreover, slightly higher oxidation potential of 1,4 dioxane ($\sim 4.78 \text{ V vs. Li/Li}^+$) compared to that of the DME and TEGDME ($\sim 4.6 \text{ V vs. Li/Li}^+$) which demonstrates a higher electrochemical stability of 1,4 dioxane. Hence, both physical and electrochemical properties of 1,4 dioxane with the comparison DME and TEGDME demonstrates its practicality for Li-O₂ system.

Property	Dioxane	DME	TEGDME
Boiling point (°C)	101.3	85	275
Melting point (°C)	11.8	-58	-30
Density (g/cm ³)	1.033	0.8683	1.009
Dielectric constant	2.21	7.2	21.26
Ionic conductivity (mS cm ⁻¹ at 40°C)	0.51	6.79	1.97

Figure 4.2 Physical property comparison of 1,4 dioxane with the most commonly used electrolytes in Li-O₂ system.

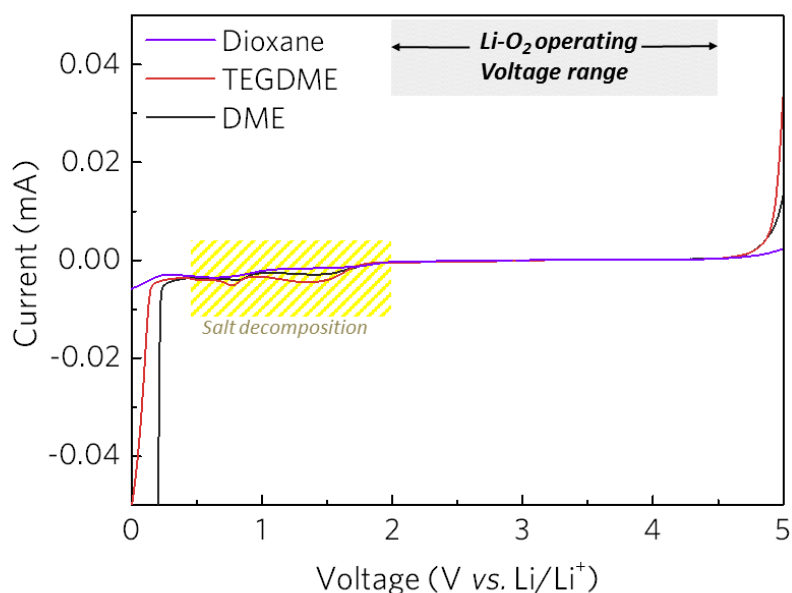


Figure 4.3 Linear sweep voltammetry (LSV) performed using the Three-electrode cell within the 0–5.0 V vs. Li/Li⁺ range at 1.0 mV s⁻¹ at 40°C. Shaded region refers to the salt decomposition²⁰.

4.2 Chemical and Electrochemical stability of Dioxane with Li metal

Previous reports has demonstrated that the electrolytes in Li-O₂ are susceptible to chemically react with Li metal⁵. Hence, many reported electrolytes such as DMSO, DMA, MeCN are not suitable for Li metal based Li-O₂ system if no other additives such as LiNO₃ salt or high concentrated lithium salt are employed^{21, 22}. Therefore, it is crucial to understand the chemical stability of electrolytes toward Li metal for the realization of Li-O₂ battery.

Figure 4.4 shows the photographs of Li metal immersed in 0.5 M LiTFSI 1,4 dioxane, DME and TEGDME electrolytes at 40°C. No sign of instant reactions such as bubbles were observed when the Li metal were in contact with the 1,4 dioxane electrolyte. Furthermore, shiny Li metal surface was sustained even after 6 days of storage. Instead, the surface of Li metal started to darken when it was immersed in 0.5 M LiTFSI TEGDME. Hence, 0.5 M LiTFSI Dioxane electrolyte has shown to be relatively stable towards Li metal compared to that of TEGDME which is one of the most commonly used electrolyte in Li-O₂ battery.

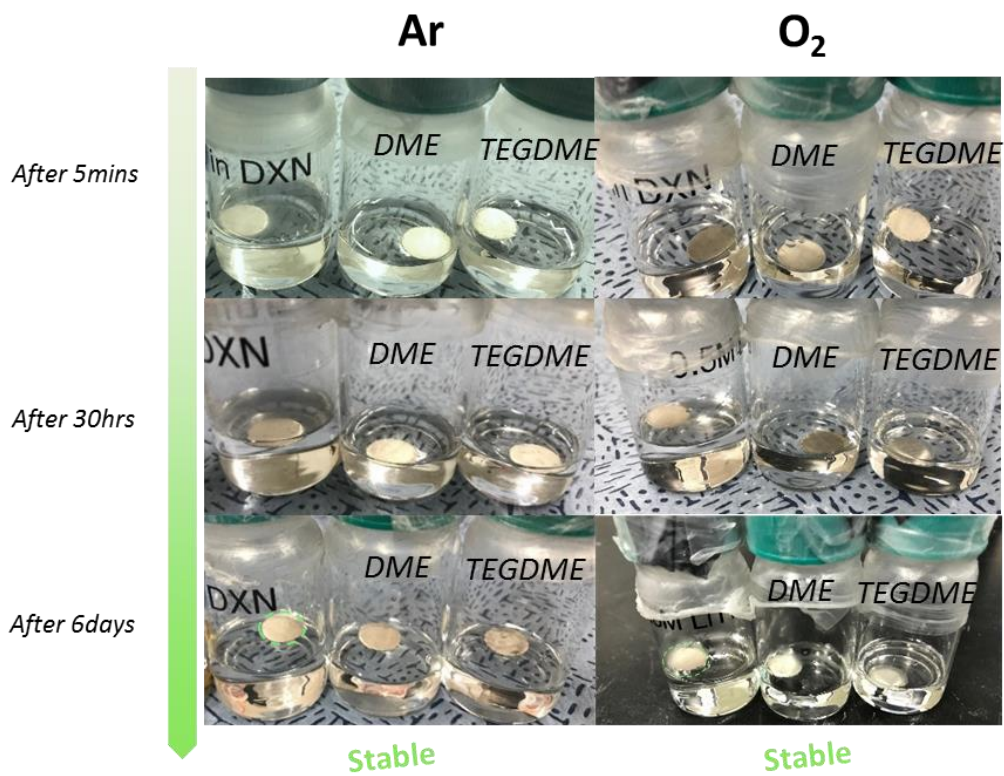


Figure 4.4 Photographs of Li metal immersed in 0.5 M LiTFSI Dioxane, DME, TEGDME at 40°C over storage time.

The stability of Dioxane towards Li metal was further examined under electrochemical cycling of Li/Li symmetric cell using 0.5 M LiTFSI Dioxane electrolyte, as shown in Figure 4.5. A larger polarization was observed for the Dioxane-based electrolyte cell compared to that of the DME-based, expecting that the lower ionic conductivity of Dioxane electrolyte is the major cause to such phenomenon. Nevertheless, similar polarization was achieved for Dioxane electrolyte compared to TEGDME. Moreover, short-circuit for TEGDME and DME occurred much earlier of ~150 hours (60 cycles) and ~320 hours (130 cycles), respectively. However, Li/Li symmetric cell with Dioxane based electrolyte has shown superior cycling stability towards Li metal of over ~550 hours (230 cycles). To examine if the superior stability towards Li metal of Dioxane based electrolyte is solely from the effect of O₂, Li/Li symmetric cell in both Ar and O₂ atmosphere has been observed for Dioxane electrolyte as shown in Figure 4.6. A smaller polarization in O₂ atmosphere was examined, and we expect that this effect is probably due to the formation of larger content of Li₂O, a well-known SEI layer which might have positive effect towards polarization. The surface morphology of Li metal in TEGDME and DME based cell was examined through SEM as shown in Figure 4.7. Noticeably, a large amount of dendritic morphology of Li was formed over the entire surface of the Li metal for TEGDME based cell, whereas a combination of mossy-like Li and dendritic Li was formed in DME. These results indicate that the Dioxane based electrolyte has superior stability towards Li metal, and opens up the possibility for the use as electrolyte in all Li metal-based battery.

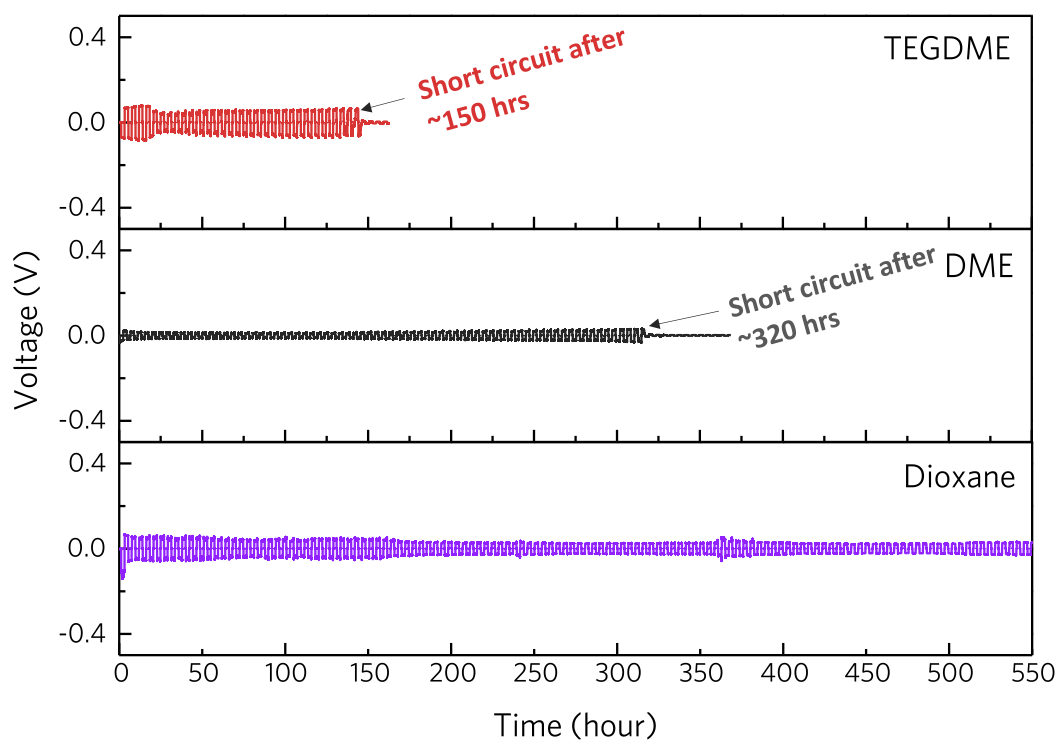


Figure 4.5 Comparison of the voltage profiles of the Li/Li symmetric cell with 0.5 M LiTFSI TEGDME, DME and Dioxane.

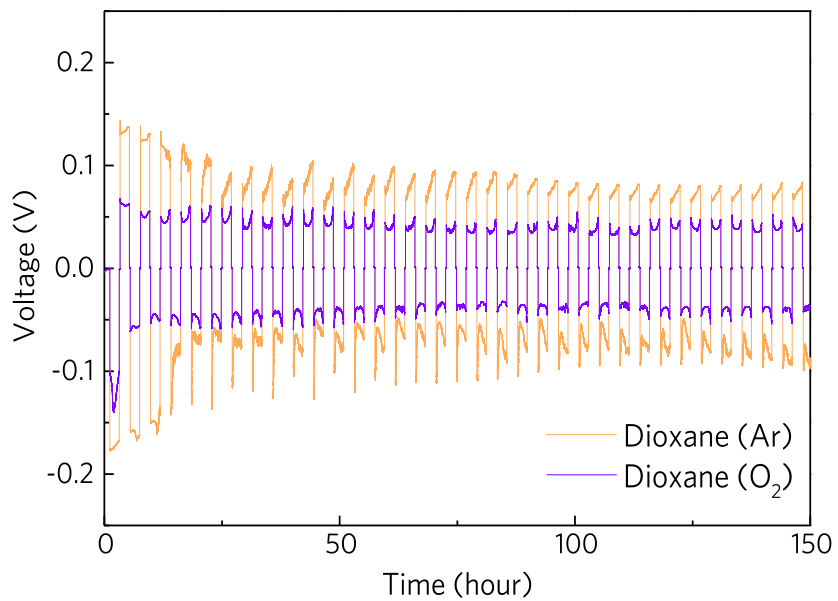


Figure 4.6 Comparison of the voltage profiles of the Li/Li symmetric cell with 0.5 M LiTFSI Dioxane in Ar and O₂ atmosphere.

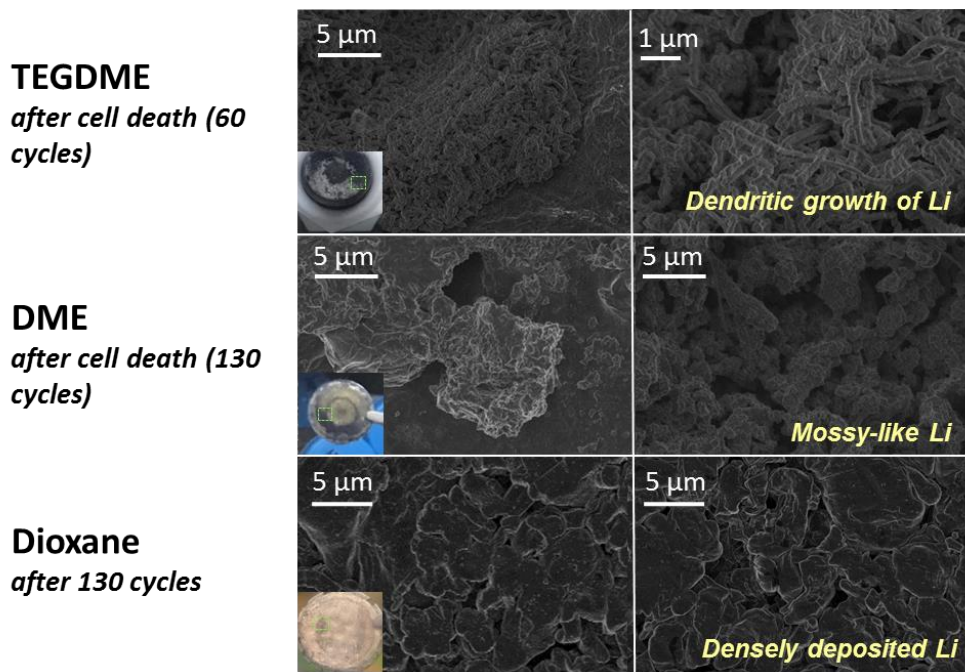


Figure 4.7 SEM images of the surface morphologies of lithium metals in 0.5 M LiTFSI TEGDME after 60 cycles, in 0.5 M LiTFSI DME and Dioxane after 130 cycles at a current density of 0.5 mA cm^{-2} .

4.3 Electrochemical profile and discharge product analysis of Dioxane

The electrochemical profile of Li-O₂ cell using 0.5 M LiTFSI in Dioxane is shown in Figure 4.8. The discharge and charge voltage profile shows typical formation and decomposition of Li₂O₂. Clearly, a higher overpotential occurs during the charging reaction indicating the sluggish kinetics of the decomposition reaction of Li₂O₂ due to its insulating nature².

Ex situ XRD and FTIR were performed to analyze the structural and chemical composition of the discharge and charge product in Dioxane based Li-O₂ cell. As shown in Figure 4.9, the reversible formation and decomposition of Li₂O₂ of Li-O₂ cell with Dioxane electrolyte clearly shows the reversibility of the system with the main discharge product of Li₂O₂. FTIR spectra in Figure 4.10 shows the main discharge product is Li₂O₂, though a slight sign of side product is observed¹⁴.

Morphological observation after discharge and charge of Dioxane based Li-O₂ cell was examined by FE-SEM and the clear toroidal Li₂O₂ formation and decomposition during discharge and charge reaction is observed²³. Hence, the structural and morphological analysis shows the reversibility and the feasibility of Dioxane electrolyte was confirmed.

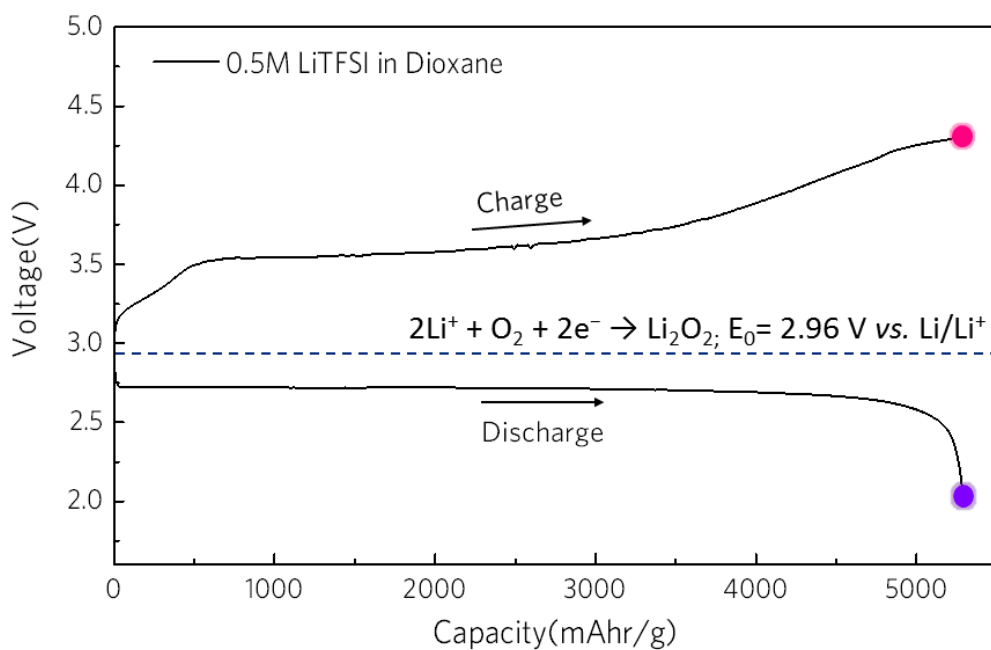


Figure 4.8 Electrochemical profile of Li-O₂ cell using 0.5 M LiTFSI in Dioxane at 0.1 mA cm⁻² at 40°C. The dotted line indicate the theoretical formation voltage of Li₂O₂. Purple and Pink circles indicate the full discharge and full charged state of the cell, respectively.

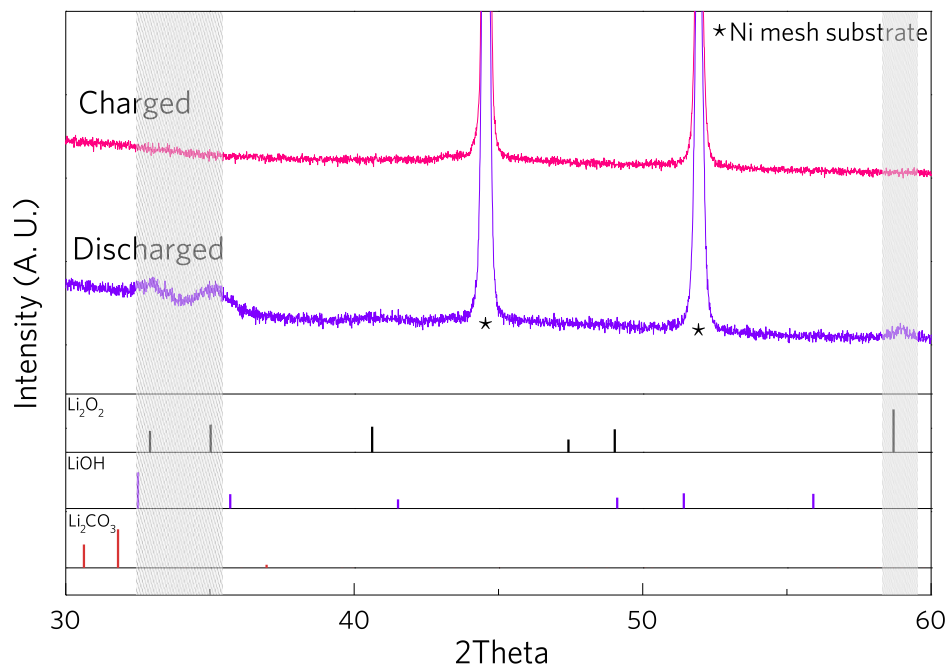


Figure 4.9 *Ex situ* XRD patterns of Li–O₂ cells using 0.5 M LiTFSI Dioxane: after discharge, and charge.

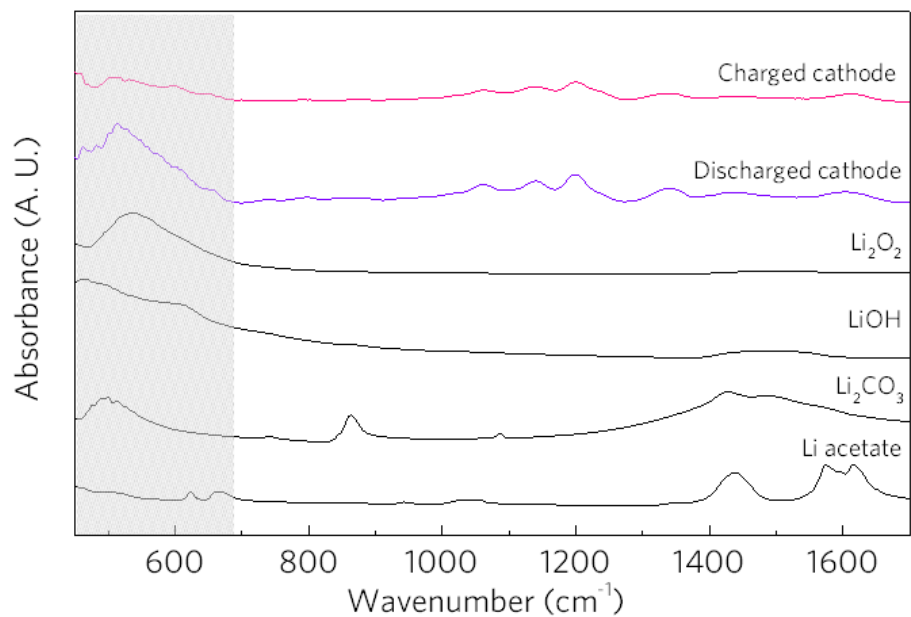


Figure 4.10 FTIR spectra of Ketjen Black cathode in 0.5 M LiTFSI in Dioxane after discharge and charge under O₂ between 2 and 4.5 V vs. (Li/Li⁺).

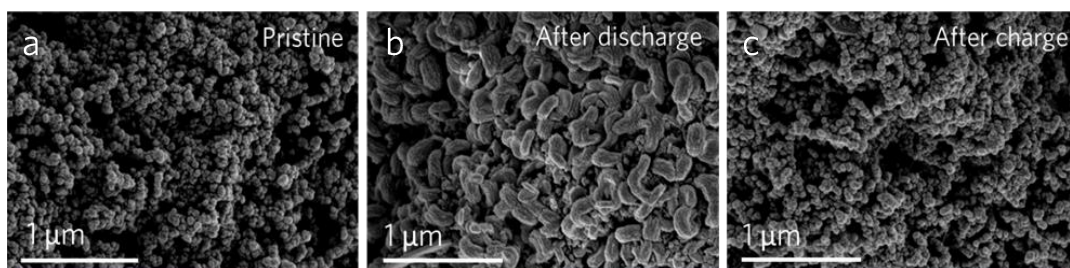


Figure 4.11 FE-SEM images of the air electrode: pristine (a), and after discharge (b) and re-charge (c) at the same magnification.

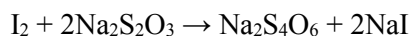
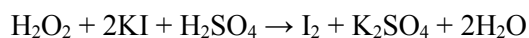
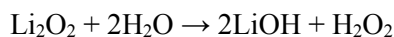
4.4 Qualitative and Quantitative study of the discharged products

In order to understand the selectivity/stability of the discharge process in Dioxane based electrolyte, qualitative and quantitative studies has been performed using UV/Vis spectroscopy and Iodometric titration technique, respectively. Alkali-metal peroxides and super oxides react with water to form hydrogen peroxide as follows¹⁸:



In order to analyze the yield of Li_2O_2 from a discharged cathode, an aqueous solution of Ti(IV)OSO_4 was used as previously reported¹⁸. Soaking the discharged cathode in H_2O will form H_2O_2 and hence the formation of $\text{H}_2[\text{Ti}(\text{O}_2)(\text{SO}_4)_2]$ complex, the former colorless solutions turn yellow with absorbance at around 407 nm¹⁸. By immersing discharged cathodes of various electrolyte at the same state of discharge into the test solution, the yield of discharge product Li_2O_2 can be qualitatively analyzed using the absorbance of UV/vis spectra. As shown in Figure 4.12, the amount of Li_2O_2 produced at fixed discharge capacity (1.0 mAh) was highest in DME, and lowest in TEGDME indicating Dioxane having relatively stable reactivity towards O_2^- compared to those of the already reported electrolytes for Li-O_2 cell.

Iodometric titration was conducted to quantify the precise yield of Li_2O_2 for Dioxane electrolyte during the discharge with the comparison of DME and TEGDME. There is a similarity between the UV/vis spectroscopy method and the iodometric titration technique which both quantifies the amount of hydrogen peroxide after reacting Li_2O_2 with water. The experimental scheme is shown as follows:



Iodine can then be titrated using a standardized sodium thiosulfate ($\text{Na}_2\text{S}_2\text{O}_3$) solution and the titration of Li_2O_2 powder (Alfa Aesar, ~95% purity) was performed in prior to the actual experiment. The detected amount of Li_2O_2 in the commercial Li_2O_2 powder was around ~92% ($\pm 2.5\%$) which indicates the reliability of such method for Li_2O_2 quantification.

The yield of discharge product Li_2O_2 in DME, Dioxane and TEGDME measured using iodometric titration is shown in Figure 4.13. The mean value of each Li_2O_2 yield was obtained through 3 repeated trials, and the mean value of DME, Dioxane and TEGDME were 73%, 69% and 64%, respectively. The two titration techniques indicate that the Dioxane electrolyte yields comparable amount of Li_2O_2 during the discharge¹⁸. In fact, DME electrolyte has been reported to achieve the

highest Li_2O_2 yield so far in organic based electrolytes. The comparable yield of Li_2O_2 obtained in Dioxane electrolyte indicates relatively stable electrolyte towards reduced oxygen species (O_2^-) and feasible to be used for Li- O_2 cell.

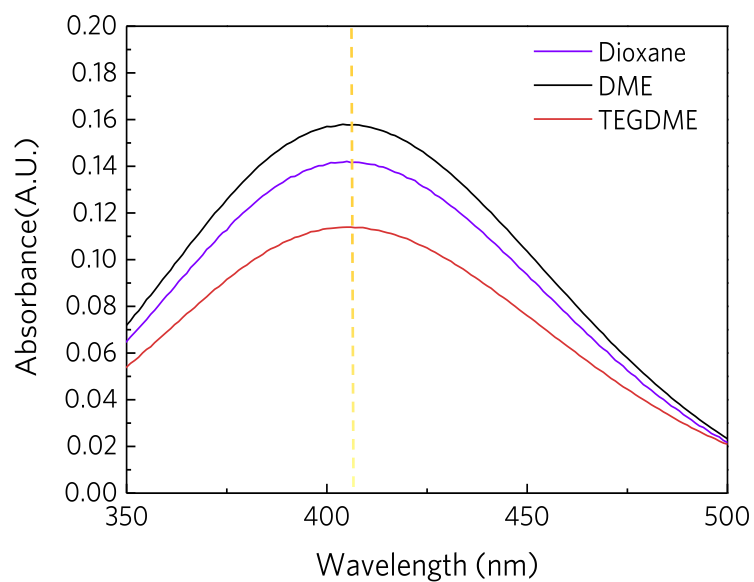


Figure 4.12 UV-vis spectra for qualitative analysis of the Li_2O_2 yield in DME, Dioxane, TEGDME. Yellow dotted line indicates the $[\text{Ti}(\text{O}_2^{2-})]^{2+}$ complex due to the presence of H_2O_2 ($\sim 407\text{nm}$)¹⁸.

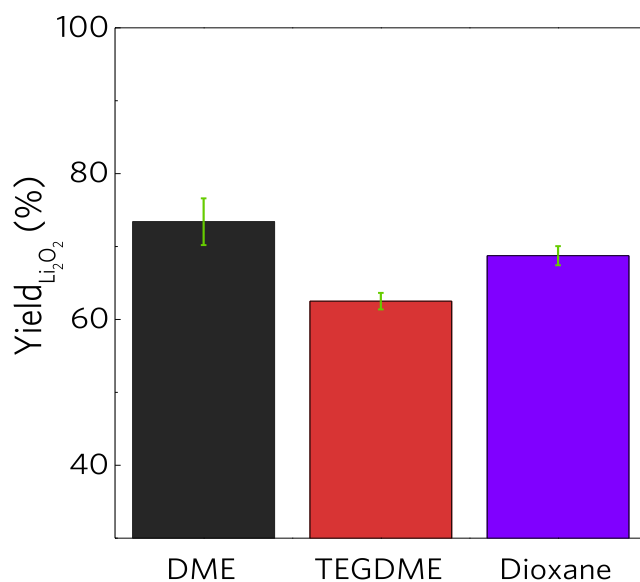


Figure 4.13 The yield of Li_2O_2 as measured by iodometric titration in different electrolytes. The yield is presented as the percentage of the expected theoretical amount on the basis of the e^- passed. Data are represented as mean \pm standard deviation.

Further investigations on quantifying the side-products after the discharge for DME, Dioxane and TEGDME has been performed as shown in Figure 4.14. By adding H_3PO_4 solution into the closed vial with discharged cathodes, CO_2 evolves from carbonate (Li_2CO_3) at very acidic condition ($\text{CO}_3^{2-} \rightarrow \text{HCO}_3^- \rightarrow \text{CO}_2$) and the quantification of CO_2 evolution directly refers to the side-products formed during the discharge due to the nucleophilic attack of the O_2^- towards electrolytes⁶. Hence, CO_2 evolution via acid treatment has long been studied previously^{6, 11}. Figure 4.14 shows the CO_2 evolution after acid treatment of discharge cathodes in DME, Dioxane and TEGDME and the amount of CO_2 evolved shows a good agreement with the result from titration of Li_2O_2 .

The overall formation of Li_2O_2 and side-products (Li_2CO_3) has been further confirmed through *in situ* DEMS. Since the DEMS analysis of O_2 and CO_2 evolution is detected while the operation of Li-O_2 cell occurs, the decomposed amount of both Li_2O_2 and side-products during the charge can be obtained. Figure 4.15 shows the DEMS analysis of DME, Dioxane and TEGDME during the charge and the ratio of O_2 to CO_2 matches well with the previous quantification results. The systematic experimental results indicate that the Dioxane electrolyte are one of the promising electrolyte for the Li-O_2 system with a higher amount of Li_2O_2 and lesser amount of side-products (Li_2CO_3) formed during the discharge compared to the widely used TEGDME electrolyte.

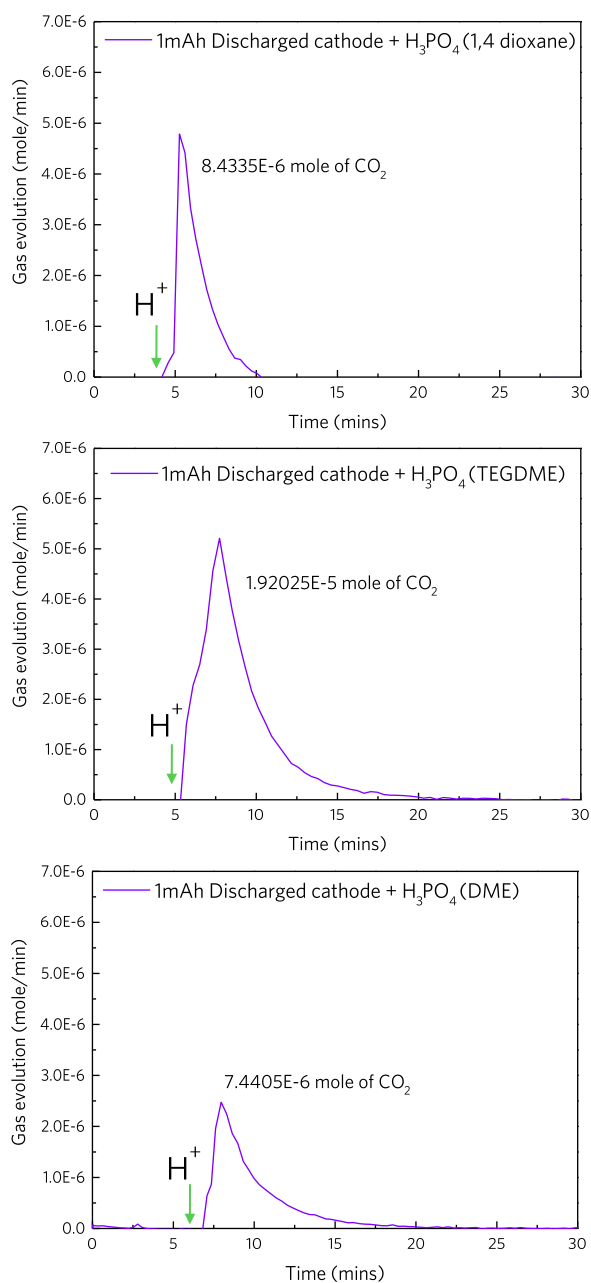


Figure 4.14 Direct comparison of the CO_2 evolution from decomposition of Li_2CO_3 (formed from decomposition of the electrolyte). H^+ indicates the time H_3PO_4 added and the evolve gas is CO_2 from Li_2CO_3 .

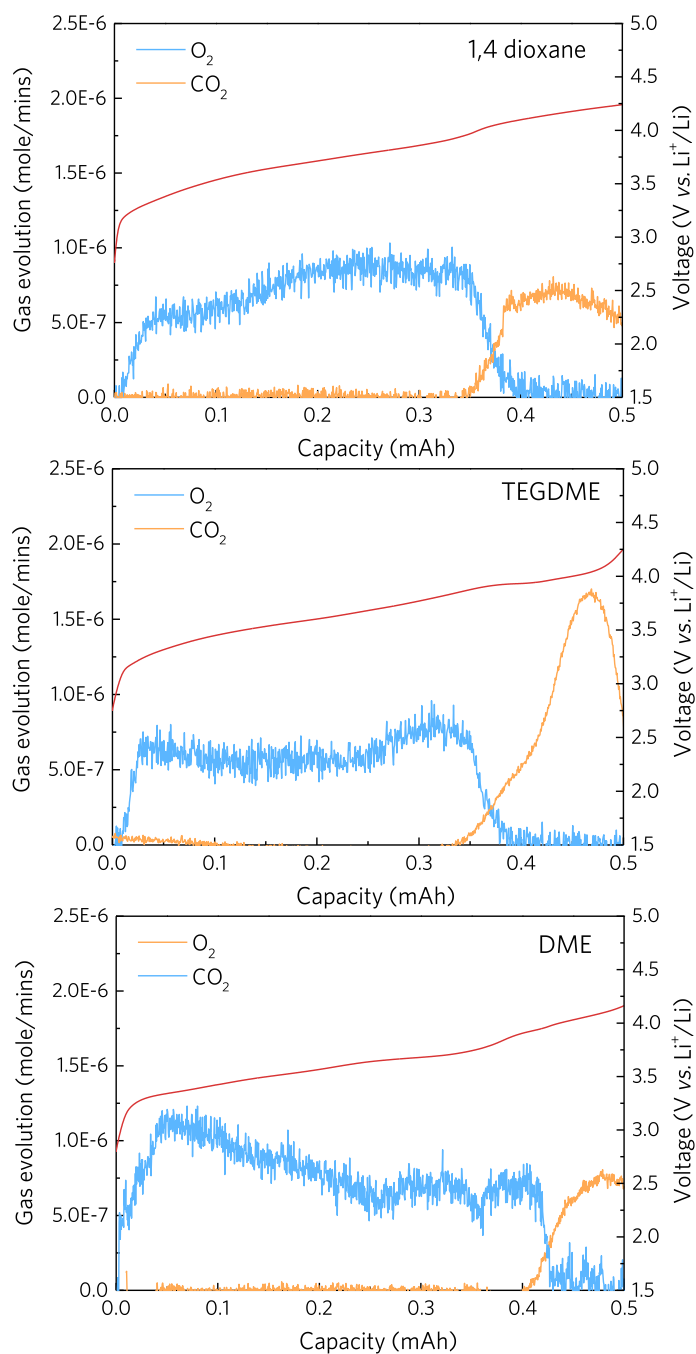


Figure 4.15 In situ DEMS analyses using Dioxane, DME and TEGDME.

4.6 Cycle performance of Dioxane electrolyte in Li-O₂ cell

To verify the performance of Dioxane electrolyte in Li-O₂ cell, cycle test of Li-O₂ cells with DME, Dioxane and TEGDME were subjected to constant-current discharge/charge at limited capacity of 500 mAh g⁻¹. As shown in Figure 4.16, a slightly larger overpotential were observed in Dioxane electrolyte compared to TEGDME and DME which presumably due to its lower ionic conductivity and not due to the amount of side-products during the discharge. The cycle performance of Dioxane electrolyte achieved a similar cycle life of ~15 cycles to that of 12, 11 cycles for DME and TEGDME, respectively. We expected that the cycle degradation occurred solely from the cathode side, since the lower utilization of Li (~1%) to that of cathode (~10%) seemed to be stable at earlier cycles in our Li/Li symmetric cell experiment. Hence, rebuilt cell with a fresh Li metal for all the electrolytes were performed as shown in Figure 4.17. Severe cycle degradation without achieving a full capacity at the 1st cycle indicated that the cycle death from the previous cells were solely due to the cathode passivation. As shown in Figure 4.18, the possible reason behind the cycle degradation might be due to accumulation of partially decomposed side-products upon cycling and therefore, we believe that the design of stable electrolytes towards reduced oxygen species must be carried on for the realization of Li-O₂ battery.

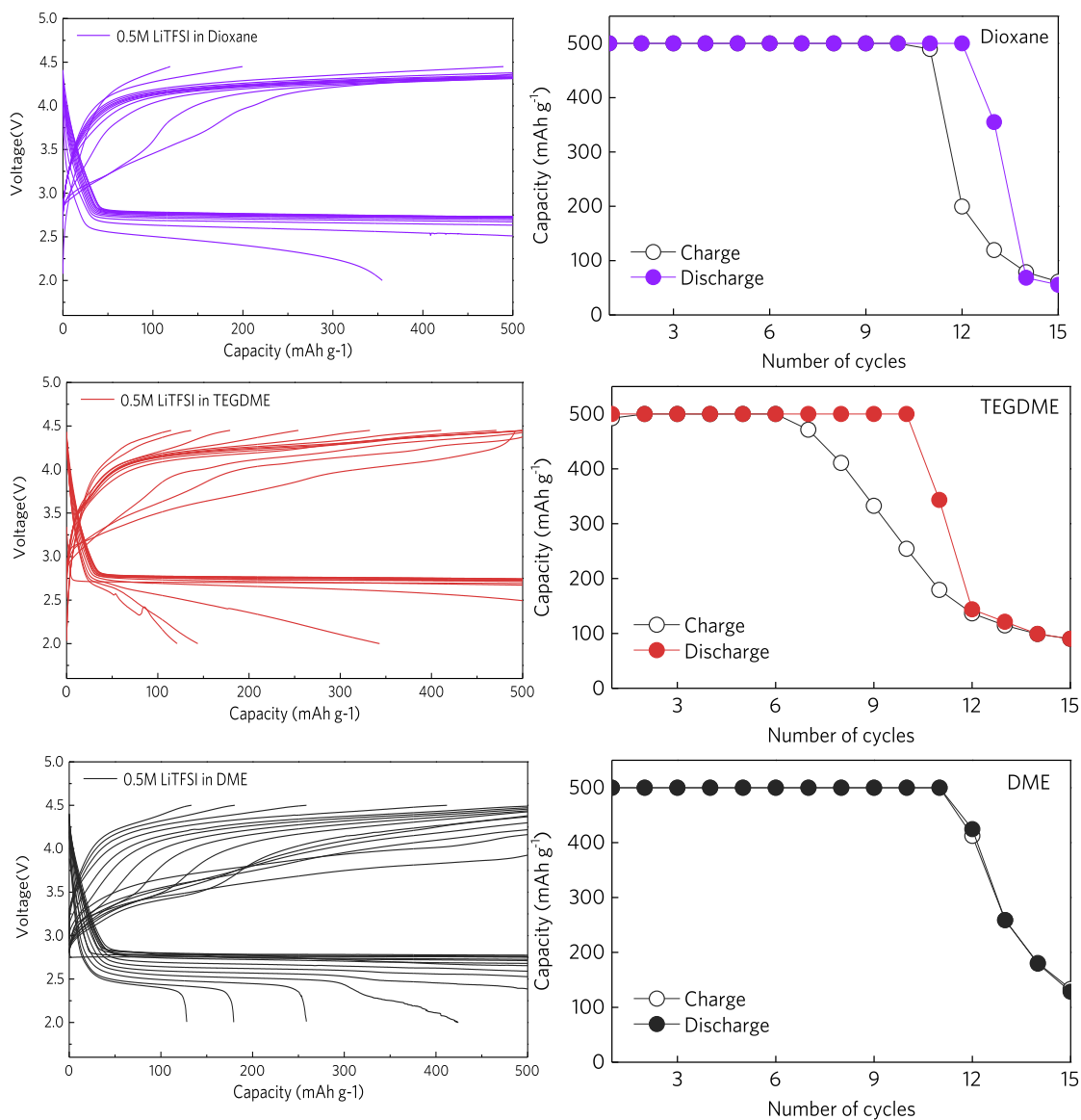


Figure 4.16 Cycling curves and capacity retention of DME, Dioxane and TEGDME Li-O₂ cell. a,b,c Galvanostatic discharge/charge cycles recorded in 0.5M LiTFSI in DME, Dioxane and TEGDME at 0.1 mA cm⁻². d,e,f Capacity retention for the same cell as in a,b,c

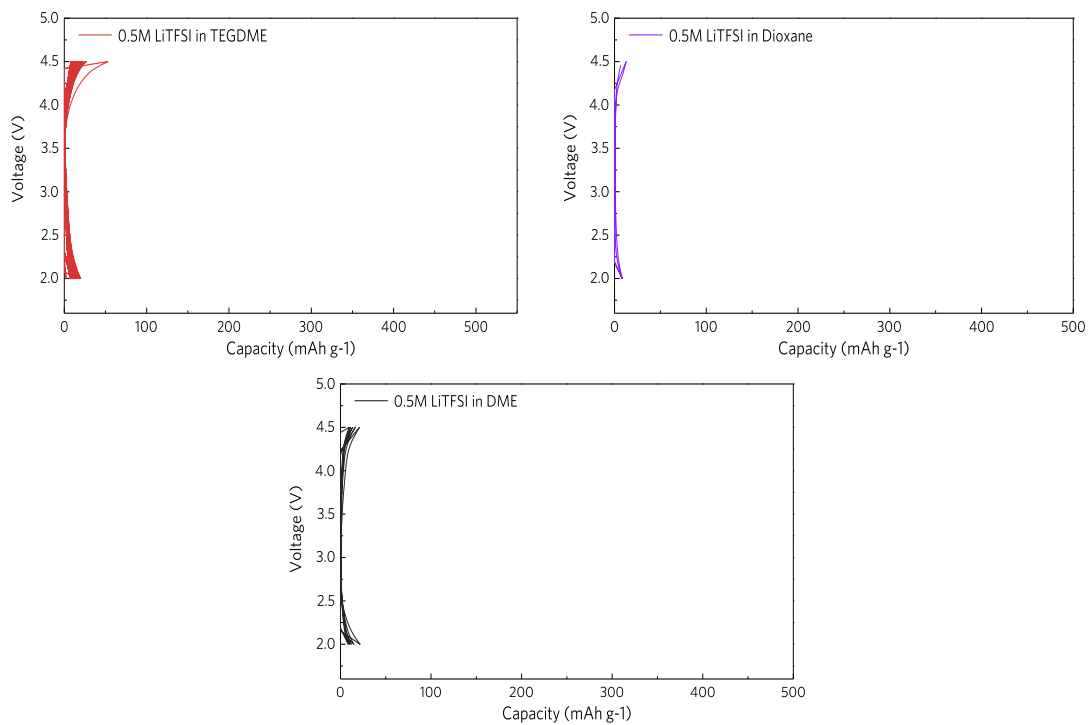


Figure 4.17 Cycling curves of DME, Dioxane and TEGDME Li-O₂ cell. Rebuilt with a fresh Li metal.

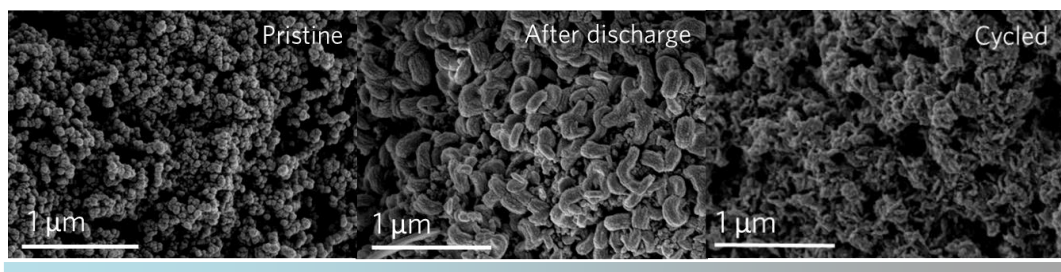


Figure 4.18 FE-SEM images of the air electrode: pristine (a), and after discharge (b) and after 15 cycles (c) at the same magnification.

Chapter 5. Conclusion

In conclusion, the electrolyte for the Li-O₂ battery has been systematically studied by understanding the stability of electrolyte towards Li metal and the cathode. We suggest that the 1,4 dioxane based electrolyte to be one of the promising electrolyte for Li-O₂ system. From the chemical and electrochemical test for Li metal stability, the superior stability of Dioxane electrolyte towards Li metal (over ~550 hours; 230 cycles) were observed. For the structural and morphological analysis, both XRD, FTIR revealed the reversible formation and decomposition of Li₂O₂ in Dioxane electrolyte were observed and toroidal-Li₂O₂ were observed from FE-SEM. Both qualitative and quantitative analysis of the discharge product, both Li₂O₂ and side-product were determined through UV/Vis spectroscopy, Iodometric titration technique, Mass Spectroscopy of CO₂ evolution after acid treatment and *in situ* DEMS analysis revealed that the relatively stable towards O₂⁻ of Dioxane electrolyte were observed.

Although few disadvantages of Dioxane electrolyte such as low ionic conductivity and higher operation temperature (40°C), Dioxane based Li-O₂ has shown comparable performance to that of currently used electrolytes in Li-O₂. With the capability of operating at a larger voltage window, and the remarkable stability towards Li metal, Dioxane electrolyte opens up a new possibility as electrolyte for highly efficient Li-O₂ battery with good Li metal and O₂⁻ stability.

Reference

1. Lim, H.-D.; Lee, B.; Bae, Y.; Park, H.; Ko, Y.; Kim, H.; Kim, J.; Kang, K. J. C. S. R., Reaction chemistry in rechargeable Li–O₂ batteries. **2017**, *46* (10), 2873-2888.
2. Bruce, P. G.; Freunberger, S. A.; Hardwick, L. J.; Tarascon, J.-M. J. N. m., Li–O₂ and Li–S batteries with high energy storage. **2012**, *11* (1), 19.
3. Lim, H. D.; Park, K. Y.; Song, H.; Jang, E. Y.; Gwon, H.; Kim, J.; Kim, Y. H.; Lima, M. D.; Robles, R. O.; Lepró, X. J. A. M., Enhanced Power and Rechargeability of a Li–O₂ Battery Based on a Hierarchical-Fibril CNT Electrode. **2013**, *25* (9), 1348-1352.
4. Freunberger, S. A.; Chen, Y.; Peng, Z.; Griffin, J. M.; Hardwick, L. J.; Bardé, F.; Novák, P.; Bruce, P. G. J. J. o. t. A. C. S., Reactions in the rechargeable lithium–O₂ battery with alkyl carbonate electrolytes. **2011**, *133* (20), 8040-8047.
5. Lee, D. J.; Lee, H.; Song, J.; Ryou, M.-H.; Lee, Y. M.; Kim, H.-T.; Park, J.-K. J. E. C., Composite protective layer for Li metal anode in high-performance lithium–oxygen batteries. **2014**, *40*, 45-48.
6. Ottakam Thotiyl, M. M.; Freunberger, S. A.; Peng, Z.; Bruce, P. G. J. J. o. t. A. C. S., The carbon electrode in nonaqueous Li–O₂ cells. **2012**, *135* (1), 494-500.
7. Reddy, D. L. a. T. B., *Handbooks of Batteries*,. McGraw-Hill: 2001; Vol. 15, p 11661-11672.
8. Aurbach, D.; McCloskey, B. D.; Nazar, L. F.; Bruce, P. G. J. N. E., Advances in understanding mechanisms underpinning lithium–air batteries. **2016**, *1* (9), 16128.
9. Lu, Y.-C.; Gallant, B. M.; Kwabi, D. G.; Harding, J. R.; Mitchell, R. R.;

- Whittingham, M. S.; Shao-Horn, Y. J. E.; Science, E., Lithium–oxygen batteries: bridging mechanistic understanding and battery performance. **2013**, *6* (3), 750-768.
10. Khetan, A.; Luntz, A.; Viswanathan, V. J. T. J. O. P. C. I., Trade-offs in capacity and rechargeability in nonaqueous Li–O₂ batteries: Solution-driven growth versus nucleophilic stability. **2015**, *6* (7), 1254-1259.
 11. McCloskey, B. D.; Valery, A.; Luntz, A. C.; Gowda, S. R.; Wallraff, G. M.; Garcia, J. M.; Mori, T.; Krupp, L. E. J. T. J. O. P. C. I., Combining accurate O₂ and Li₂O₂ assays to separate discharge and charge stability limitations in nonaqueous Li–O₂ batteries. **2013**, *4* (17), 2989-2993.
 12. Aetukuri, N. B.; McCloskey, B. D.; García, J. M.; Krupp, L. E.; Viswanathan, V.; Luntz, A. C. J. N. C., Solvating additives drive solution-mediated electrochemistry and enhance toroid growth in non-aqueous Li–O₂ batteries. **2015**, *7* (1), 50.
 13. Johnson, L.; Li, C.; Liu, Z.; Chen, Y.; Freunberger, S. A.; Ashok, P. C.; Praveen, B. B.; Dholakia, K.; Tarascon, J.-M.; Bruce, P. G. J. N. C., The role of LiO₂ solubility in O₂ reduction in aprotic solvents and its consequences for Li–O₂ batteries. **2014**, *6* (12), 1091.
 14. Freunberger, S. A.; Chen, Y.; Drewett, N. E.; Hardwick, L. J.; Bardé, F.; Bruce, P. G. J. A. C. I. E., The lithium–oxygen battery with ether-based electrolytes. **2011**, *50* (37), 8609-8613.
 15. Pohjalainen, E., *Negative Electrode Materials for Lithium Ion Batteries*. Aalto University: Department of Chemistry, 2016; Vol. 42, p 4693-4699.
 16. Abraham, K.; Jiang, Z. J. J. O. T. E. S., A polymer electrolyte-based rechargeable lithium/oxygen battery. **1996**, *143* (1), 1-5.
 17. Lim, H.-D.; Gwon, H.; Kim, H.; Kim, S.-W.; Yoon, T.; Choi, J. W.; Oh, S.

- M.; Kang, K. J. E. A., Mechanism of Co_3O_4 /graphene catalytic activity in Li-O_2 batteries using carbonate based electrolytes. **2013**, *90*, 63-70.
18. Hartmann, P.; Bender, C. L.; Sann, J.; Dürr, A. K.; Jansen, M.; Janek, J.; Adelhelm, P. J. P. C. C. P., A comprehensive study on the cell chemistry of the sodium superoxide (NaO_2) battery. **2013**, *15* (28), 11661-11672.
 19. Knipping, E.; Aucher, C.; Guirado, G.; Aubouy, L. J. N. J. o. C., Room temperature ionic liquids versus organic solvents as lithium–oxygen battery electrolytes. **2018**, *42* (6), 4693-4699.
 20. Moreno, M.; Simonetti, E.; Appetecchi, G.; Carewska, M.; Montanino, M.; Kim, G.-T.; Loeffler, N.; Passerini, S. J. J. o. T. E. S., Ionic Liquid Electrolytes for Safer Lithium Batteries I. Investigation around Optimal Formulation. **2017**, *164* (1), A6026-A6031.
 21. Walker, W.; Giordani, V.; Uddin, J.; Bryantsev, V. S.; Chase, G. V.; Addison, D. J. J. o. t. A. C. S., A rechargeable Li-O_2 battery using a lithium nitrate/N, N-dimethylacetamide electrolyte. **2013**, *135* (6), 2076-2079.
 22. Yamada, Y.; Furukawa, K.; Sodeyama, K.; Kikuchi, K.; Yaegashi, M.; Tateyama, Y.; Yamada, A. J. J. o. t. A. C. S., Unusual stability of acetonitrile-based superconcentrated electrolytes for fast-charging lithium-ion batteries. **2014**, *136* (13), 5039-5046.
 23. Adams, B. D.; Radtke, C.; Black, R.; Trudeau, M. L.; Zaghbi, K.; Nazar, L. F. J. E.; Science, E., Current density dependence of peroxide formation in the Li-O_2 battery and its effect on charge. **2013**, *6* (6), 1772-1778.

국문요약

최근 전 세계적으로 환경 문제에 대한 관심이 커지는 만큼 지구온난화를 해결할만한 에너지 시스템이 큰 관심을 받고 있다. 휴대성과 고용량의 두 가지 요소를 해결해주는 차세대 배터리 개발에 대한 관심도 커짐에 따라 기존 리튬 이온 기반의 배터리를 대체할 수 있는 배터리 시스템 중 리튬-공기 전지가 큰 관심을 끌고 있다. 리튬/공기 전지는 높은 이론 용량으로 미래 에너지 응용 분야에서 가장 큰 가능성을 가지고 있다⁷. 그러나 높은 과전압, 배터리 수명 저하 등 많은 문제들이 제기되어 왔다^{2, 3, 5, 6, 14}. 특히 리튬-공기 전지의 전기화학 반응 중 생성되는 활성 산소(O_2^-)의 화학적 불안정성으로 인해 전지의 성능이 저하되는 문제는 현재까지도 해결되지 않은 문제로 대두되고 있다. 또한 리튬-공기에서 필히 사용되는 음극인 리튬 금속과 전해질의 불안정성 또한 반복적 사이클을 견디지 못하고 수지상 성장을 일으킨다. 이러한 문제점들을 극복하기 위하여 본 연구에서는 안정하고 부반응이 적은 새로운 리튬-공기용 전해질 후보군들을 제안했다.

본 연구는 화학적과 전기화학적 접근을 통해 새로운 유기전해질과 활성산소(O_2^-) 및 리튬 금속에 대한 안정성을 실험적으로 검증하였으며, 리튬-공기용 전해질로써의 그 실현 가능성을 검토하였다. 비교군들과의 결과를 비취보았을 때, 본 연구에서 제안하는 전해질은

높은 리튬 금속과의 안정성을 보였으며, 높은 수율의 과산화리튬을 통해 활성 산소와의 안정성을 밝혀냈다. 또한, 그 수준이 현재 보고된 리튬-공기 전지용 전해질과 유사한 수준을 보이는 것을 검증했다. 그럼에도 불구하고, 반복적 사이클에서는 완전히 분해되지 않은 부반응의 축적으로 기존 리튬-공기 전지용 전해질과 동일한 원인에 의해 수명이 다하는 것을 확인할 수 있었다. 따라서, 본 연구를 통해 안정한 전해질을 찾는 것이 매우 중요하다는 것을 제기하였으며, 앞으로도 지속적인 안정성 연구를 통해 리튬-공기 전지를 실현하는 날이 올 것이다.

주요어: 리튬-공기 전지, 유기 전해질, O_2^- 안정성, 리튬 금속과의 안정성

학 번: 2018-28630